

# Insight into Potential Well Based Nanoscale FDSOI MOSFET Using Doped Silicon Tubs- A Simulation and Device Physics Based Study: Part I: Theory and Methodology

Shruti Mehrotra, S. Qureshi

Department of Electrical Engineering, Indian Institute of Technology Kanpur, India

---

## Abstract

A novel planar device having doped silicon regions (tubs) under the source and drain of an FDSOI MOSFET is reported at 20 nm gate length. The doped silicon regions result in formation of potential wells (PW) in the source and drain regions of FDSOI MOSFET and thus, the device being called as Potential Well Based FDSOI MOSFET (PWFDSONI MOSFET). Simulation and device physics study on PWFDSONI MOSFET showed reduction in the OFF current of the device by orders of magnitude. A low  $I_{OFF}$  of 22 pA/ $\mu\text{m}$ , high  $I_{ON}/I_{OFF}$  ratio of  $1.5 \times 10^7$  and subthreshold swing of 76 mV/decade were achieved in 20 nm gate length PWFDSONI MOSFET. The study was performed on devices with unstrained silicon channel.

**Keywords:** FDSOI MOSFET, Ground plane,  $I_{ON}/I_{OFF}$ , Planar, Potential well, PWFDSONI MOSFET

---

## 1. Introduction

The recent past has witnessed aggressive scaling of the technology node in a bid to meet Moore's law. This scaling has caused reduced gate control which consequently leads to high OFF current ( $I_{OFF}$ ) and poor subthreshold swing (SS) [1]. Studies have reported devices like FinFET, TFET and the concept of negative capacitance to overcome these short comings [2, 3, 4, 5, 6, 7]. Even though FinFET offers excellent gate control, being a 3D device it has process and design level complexities. While NCFET improves SS with increasing thickness of the ferroelectric layer, it suffers from hysteresis [8]. The Fully Depleted Silicon-on-Insulator (FDSOI) MOSFET continues to be an attractive device option because of its planar topology and back-biasing feature. We have recently reported a novel Potential Well Based FDSOI MOSFET (PWFDSONI MOSFET) at 10 nm gate length to achieve a high ON-to-OFF current ratio ( $I_{ON}/I_{OFF}$ ) [9]. In this paper, we explore the details of formation of potential wells at 20 nm gate length in the source and drain regions due to the introduction of heavily

doped silicon regions in the BOX under the source and drain. The paper is based on simulation studies supported by p-n junction device physics responsible for the creation of potential wells in the source/drain regions which results in significant reduction in the OFF current of the device. This paper is organised as follows: Section 2 discusses the concept of formation of potential wells in the source and drain regions and the simulation methodology followed to realize the conventional FDSOI MOSFET with ground plane (GP)(reference device in this study) and the proposed PWFDSONI MOSFET at 20 nm gate length with doped silicon regions under the source and drain in the BOX. Section 3 discusses the physics behind PWFDSONI MOSFET and Section 4 draws the conclusion.

## 2. Formation of Potential Wells

We report a novel approach to create potential wells in the source and drain regions of PWFDSONI MOSFET by introducing doped silicon regions in the buried oxide under the source and drain regions. This study was performed on devices with unstrained silicon channel.

---

\*Corresponding author

Email address: mshruti@iitk.ac.in (Shruti Mehrotra)

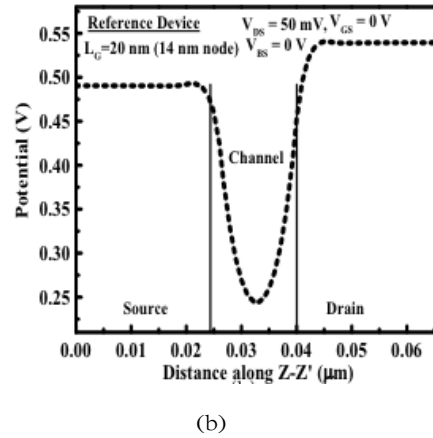
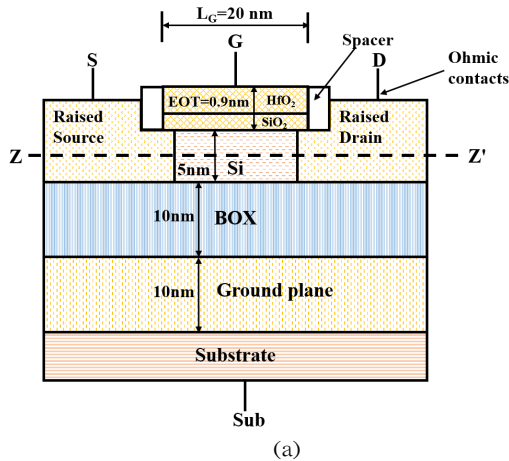


Fig. 1: (a) Schematic of 20 nm FDSOI MOSFET with  $p^+$  ground plane (GP) under the BOX. The horizontal cutline Z-Z' is drawn in the center of the channel (2.5 nm from the gate stack/channel interface). (b) Relative channel potential profile in FDSOI MOSFET with GP in OFF state ( $V_{GS} = 0$  V). Absence of potential wells in source and drain regions in 20 nm FDSOI MOSFET is observed.

Table 1: Models used in 2D TCAD simulations of FDSOI MOSFET

TCAD Models	Physical Effect Captured
Drift Diffusion	Carrier transport
SRH and Auger	Carrier recombination
Quantum confinement	SOI layer is very thin leading to quantum confinement of carriers
Lombardi mobility model	Acoustic phonon scattering at low fields and surface recombination scattering at high transverse fields
High field mobility model	Velocity saturation effect
Self heating model	Lattice heating in the SOI layer
Fermi Dirac carrier statistics	Presence of heavily doped regions in the device
Bandgap narrowing	At very high doping in silicon, the $pn$ product becomes doping dependent

Table 2: Device Parameters used in Simulations at 20 nm Gate Length

Parameter	Value
Gate Length	20 nm
EOT	0.9 nm
HfO <sub>2</sub> thickness	3.8 nm
SiO <sub>2</sub> thickness	0.3 nm
Permittivity of HfO <sub>2</sub>	25
SOI layer thickness	5 nm
BOX thickness	10 nm
GP thickness	10 nm
Spacer length	3 nm
Gate-to-source/drain overlap	3 nm
SOI layer doping	$10^{15} \text{ cm}^{-3}$
Source/Drain doping	$10^{20} \text{ cm}^{-3}$
Ts/TD doping	$10^{20} \text{ cm}^{-3}$
Ground plane doping	$10^{20} \text{ cm}^{-3}$
Substrate doping	$10^{15} \text{ cm}^{-3}$
Work function of gate metal	4.52 eV

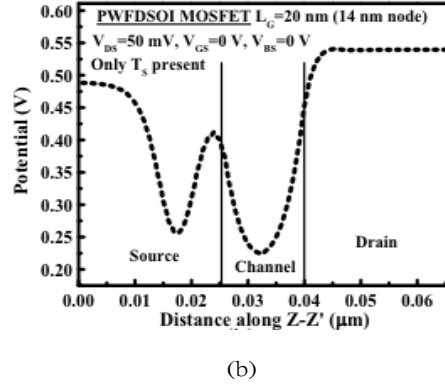
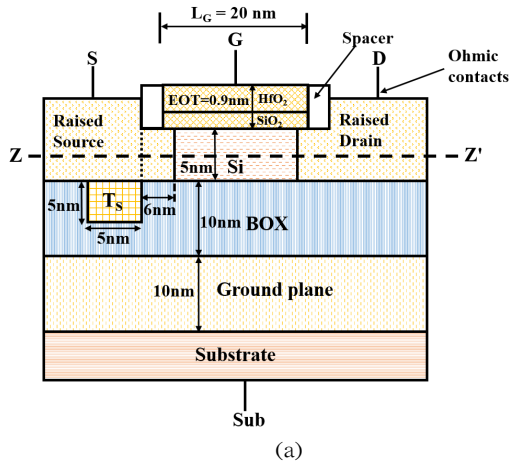


Fig. 2: (a) Schematic of 20 nm PWFDSOI MOSFET with region  $T_s$  under the source. The doping of  $T_s$  is p-type with a concentration of  $1 \times 10^{20} \text{ cm}^{-3}$ . The horizontal cutline Z-Z' is drawn in the center of the channel (2.5 nm from the gate stack/channel interface). (b) Potential well in the source region of 20 nm PWFDSOI MOSFET with region  $T_s$  under the source. The relative potential profile is plotted along cutline Z-Z' when the device is in OFF state ( $V_{GS} = 0 \text{ V}$ ).

### 2.1. Simulation Methodology and Reference Device

FDSOI MOSFET with degenerately doped ( $\sim 10^{20} \text{ cm}^{-3}$ ) region under the BOX called the ground plane (GP) was the reference device in this study [10]. First a structure as proposed in [10] was realized at 20 nm gate length for calibration. The silicon layer that forms the channel was 6 nm thick and the BOX was 25 nm thick. As a next step to realize an ultra thin body and BOX structure, the silicon layer thickness was reduced to 5 nm and the BOX thickness was reduced to 10 nm. The device had an HKMG gate stack with an EOT of 0.9 nm as shown in Fig. 1(a). The gate-to-source/drain overlap was 3 nm. This has also been confirmed through process simulations in Silvaco Athena [11]. As shown in Fig. 1(b) the relative potential profile along the cutline Z-Z' through the center of the channel shows the channel potential as expected. The simulation study was performed in Silvaco TCAD [12]. Relevant models invoked to capture the physics of the devices are mentioned in Table 1. The device parameters used in simulations are mentioned in Table 2.

### 2.2. 20 nm gate length PWFDSOI MOSFET

The proposed PWFDSOI MOSFET had heavily doped ( $10^{20} \text{ cm}^{-3}$ ) silicon regions (tubs)  $T_s$  and  $T_D$  under the source and drain respectively in the BOX. The proposed device PWFDSOI MOSFET was identical to the reference device in all respects except for the presence of the doped silicon tubs  $T_s$  and  $T_D$ . The doping of the tubs was of opposite type as compared to source/drain doping ( $p^+$

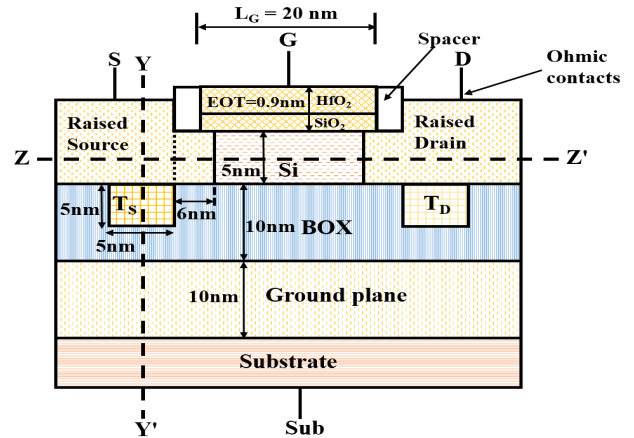


Fig. 3: 20 nm PWFDSOI MOSFET with regions  $T_s$  and  $T_D$  under the source and drain respectively. The doping of  $T_s$  and  $T_D$  is p-type with a concentration of  $1 \times 10^{20} \text{ cm}^{-3}$ . It has an HKMG gate stack with an EOT of 0.9 nm. The cutline Z-Z' is through the center of the channel.

in n-channel PWFDSOI MOSFET). These doped silicon tubs were 5 nm (depth) x 5 nm (width). As mentioned earlier, the presence of  $T_s$  and  $T_D$  leads to p-n junctions formation and consequent potential wells in the source and drain regions.

Figure 2(a) shows 20 nm PWFDSOI MOSFET when only  $T_s$  is present under the source. Relative potential profile along cutline Z-Z' for this case shows the potential well in the source only which is illustrated in Fig. 2(b). Similarly, when only  $T_D$  is present under the drain, a potential well is formed in the drain only.

The schematic of the proposed 20 nm PWFDSOI MOSFET is shown in Fig. 3. Figure 4(a) shows the potential wells in the source and drain regions for the proposed 20 nm gate length PWFDSOI MOS-



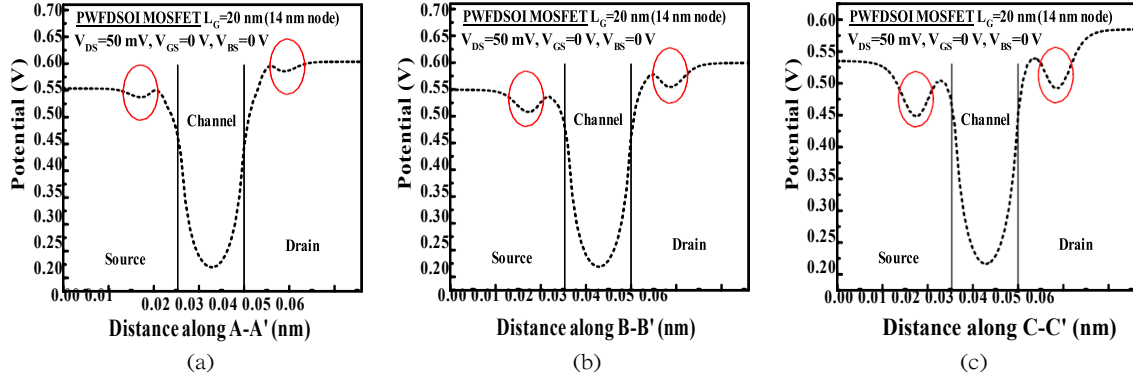


Fig. 7: (a) Relative potential profile along cutline A-A' in OFF state for 20 nm gate length PWFDSOI MOSFET. The potential well depth in the source is very small (16 meV). (b) Relative potential profile along cutline B-B' in OFF state for 20 nm gate length PWFDSOI MOSFET. The potential well depth in the source is 42 meV. (c) Relative potential profile along cutline C-C' in OFF state for 20 nm gate length PWFDSOI MOSFET. The potential well depth in the source is 86 meV. The circled portions show the potential wells in the source and drain regions.  $V_{DS} = 50$  mV,  $V_{GS} = 0$  V and  $V_{BS} = 0$  V.

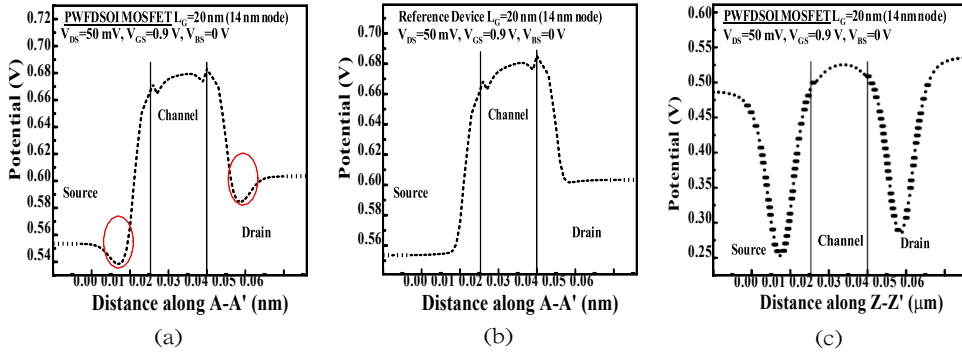


Fig. 8: (a) Relative potential profile along cutline A-A' in ON state for PWFDSOI MOSFET. The potential well depth in source and drain regions is very small. (b) Relative potential profile along cutline A-A' in ON state for reference FDSOI MOSFET. There is absence of potential wells in source and drain regions in the reference device. (c) Potential wells in source and drain regions along cutline Z-Z' in 20 nm PWFDSOI MOSFET when device is in inversion ON state.  $V_{DS} = 50$  mV,  $V_{GS} = 0.9$  V and  $V_{BS} = 0$  V.

becomes significantly large at the center along the cutline Z-Z' having a value of 225 meV as observed from Fig. 4(a). Therefore, it is reasonable to assume that primarily electrons in the top portion of the source in the vicinity of the gate contribute to the OFF current in PWFDSOI MOSFET. Under this assumption, the carrier transport mechanism remains the same as in the reference device. Thus, the drift-diffusion transport model is used in the TCAD simulations of the PWFDSOI MOSFET also under this assumption because in PWFDSOI MOSFET it is the reduction in the number of carriers contributing to the OFF current as compared to the reference device.

For PWFDSOI MOSFET in the ON state ( $V_{DS} = 50$  mV,  $V_{GS} = 0.9$  V,  $V_{BS} = 0$  V) of the device, the relative potential profile has been analysed along two cutlines, A-A' and Z-Z' as shown in Figs. 6 and 3 respectively. The relative potential

profile along cutline A-A' for PWFDSOI MOSFET in ON state is shown in Fig. 8(a). The potential well depth in the source and drain regions is very small, same as in OFF state (16 meV). The relative potential profile along the same cutline A-A' for the reference device is shown in Fig. 8(b). The relative potential profile along cutline Z-Z' in 20 nm gate length PWFDSOI MOSFET in ON state of the device is shown in Fig. 8(c). The potential well depth in the source and drain regions is more than that observed in Fig. 8(a) and is around 300 meV.

### 3. Physics of PWFDSOI MOSFET

#### 3.1. Transfer characteristics

##### 3.1.1. 20 nm gate length PWFDSOI MOSFET

The transfer characteristics of the 20 nm gate length PWFDSOI MOSFET are shown in Fig. 9 at  $V_{DS} = 0.9$  V and in the absence of a back-bias. It

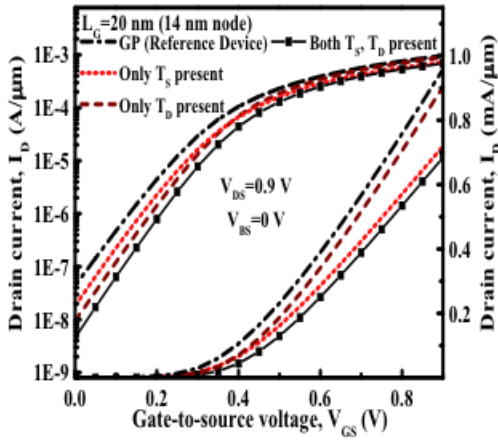


Fig. 9:  $I_D$  vs.  $V_{GS}$  characteristics of 20 nm PWFDSOI MOSFET with regions  $T_S$  and  $T_D$  under the source and drain respectively. A step-by-step comparison is drawn in the figure between reference device, either  $T_S$  or  $T_D$  present and the case when both  $T_S$  and  $T_D$  are present (proposed device).  $V_{DS} = 0.9$  V and  $V_{BS} = 0$  V.

is interesting to note that  $I_{OFF}$  ( $I_D$  at  $V_{GS} = 0$  V) when only  $T_D$  was present was less than when only  $T_S$  was present. This is because when only  $T_S$  was present, the carriers which have sufficient energy to overcome the source-to-channel barrier reach the drain terminal and contribute to  $I_{OFF}$ . On the contrary, when only  $T_D$  was present smaller  $I_{OFF}$  resulted as the carriers experienced barrier due to  $T_D$  even though more carriers from the source were expected to get into the channel. Consequently, when neither  $T_S$  nor  $T_D$  was present (Figs. 1(a) and 1(b)),  $I_{OFF}$  was maximum and when both  $T_S$  and  $T_D$  were present (Figs. 3 and 4(a)),  $I_{OFF}$  was minimum. The presence of potential wells in source and drain does not lead to a significant reduction in ON current ( $I_{ON} = I_D$  at  $V_{GS} = V_{DS}$ ) as compared to ON current of the reference device. This results in improved  $I_{ON}/I_{OFF}$  ratio for 20 nm PWFDSOI MOSFET.

Further, a back-bias of -1 V was applied to achieve better front gate control [13]. In PWFDSOI MOSFET, besides improving gate control, back-bias was seen to increase the depth of the potential wells and thus, reduction of OFF current. Figure 10 shows the transfer characteristics of the 20 nm PWFDSOI MOSFET and the reference device in the presence of back-bias. Table 3 gives the device performance parameters for 20 nm PWFDSOI MOSFET for the bias condition  $V_{DS}$  of 0.9 V and  $V_{BS}$  of -1.0 V.

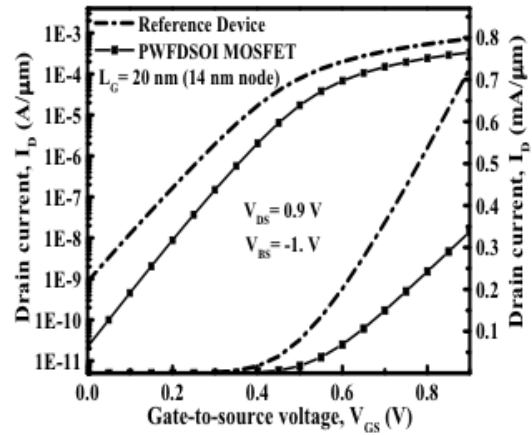


Fig. 10:  $I_D$  vs.  $V_{GS}$  characteristics of 20 nm PWFDSOI MOSFET with regions  $T_S$  and  $T_D$  under the source and drain respectively. A comparison is drawn with the reference device.  $V_{DS} = 0.9$  V and  $V_{BS} = -1.0$  V.

### 3.1.2. Physics of PWFDSOI MOSFET

### 3.2. Electric Field

The electric field profile in PWFDSOI MOSFET is altered significantly in comparison to the electric field profile of the reference device as shown in Fig. 11. This can be attributed to the presence of space charge created by the formation of the p-n junctions which makes the presence of the GP more effective in the termination of field lines. This also explains the improvement of DIBL in PWFDSOI MOSFET in comparison to GP as discussed in Part II.

### 3.3. Potential well depth as function of distance along Y-Y' in the source

The variation of depth of potential well in the source as we move from source towards source/ $T_S$  interface is shown in Fig. 12. The potential well depth increases as we move along cutline Y-Y' from a point in the source to the source/ $T_S$  interface. This can be attributed to the increased influence of the positive space charge on the carriers. Thus, electrons located deeper in the source are less likely to contribute to the OFF current. With the application of a back-bias, the potential well depth increases further causing a significant reduction in leakage current as shown in Fig. 10 and for reasons mentioned in Part II.

### 3.4. Potential variation along Y-Y'

The variation of relative potential was also studied along the cutline Y-Y' across the n-p junction formed by the source and  $T_S$  in 20 nm PWFDSOI MOSFET and is shown in Fig. 13. The study was performed under equilibrium condition

Table 3: Performance parameters at 20 nm gate length

	PWFDSOI MOSFET	Reference Device
SS (mV/decade)	76	85
$I_{OFF}$ (pA/ $\mu\text{m}$ )	22	860
$I_{ON}$ (mA/ $\mu\text{m}$ )	0.34	0.37
$I_{ON}/I_{OFF}$	$1.5 \times 10^7$	$8.4 \times 10^5$

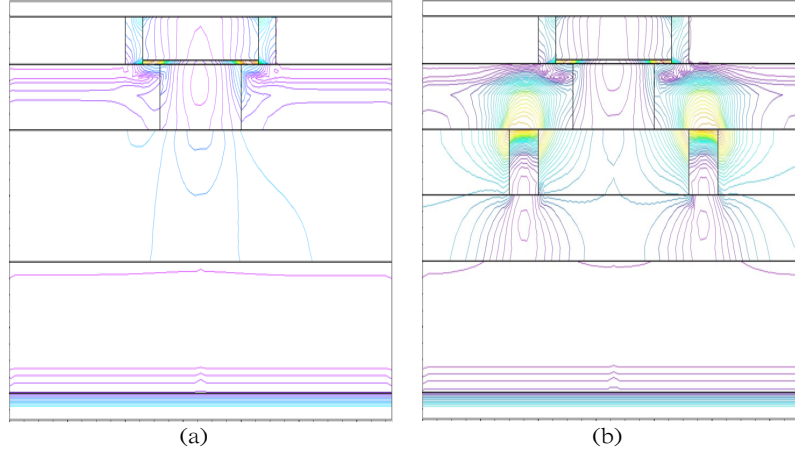


Fig. 11: Electric field profiles of (a) reference device and, (b) PWFDSOI MOSFET.  $V_{DS} = 50$  mV,  $V_{GS} = 0$  V and  $V_{BS} = 0$  V.

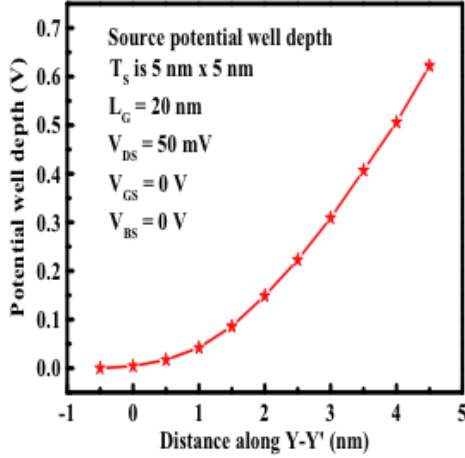


Fig. 12: Variation of potential well depth in the source in 20 nm PWFDSOI MOSFET along cutline Y-Y'. Here Y-Y' = 0 is the gate stack/channel interface as shown in Fig. 3.

( $V_{DS} = V_{GS} = V_{BS} = 0$  V). The difference in the potential across the n-p junction is approximately equal to 1.12 eV which is the band gap energy of silicon as shown in Fig. 13. Also, it is clearly observed in Fig. 13 that a significantly larger potential drop occurs in the source region and only about 2 nm depth of  $T_S$  from the source/ $T_S$  interface is depleted. This suggests significant depth of  $T_S$  region is quasi neutral. This implies that process variations in depth of the  $T_S$  and  $T_D$  will not make a

significant impact on the performance of the device.

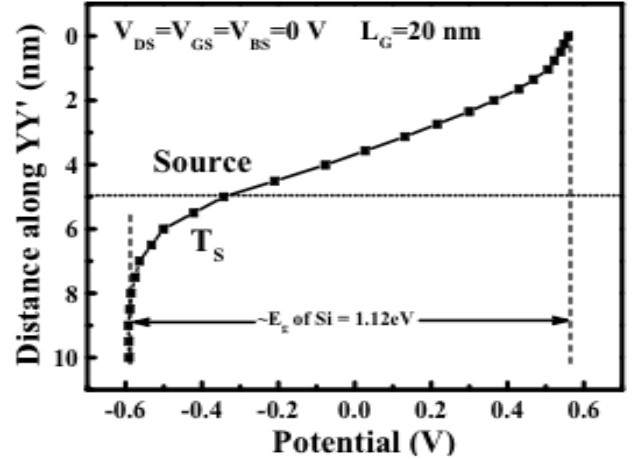


Fig. 13: Variation of relative potential from source to  $T_S$  in 20 nm PWFDSOI MOSFET under the condition:  $V_{DS} = V_{GS} = V_{BS} = 0$  V for doped silicon  $T_S$  and  $T_D$ . Here Y-Y' = 0 is the gate stack/channel interface as shown in Fig. 3.

#### 4. Conclusion

A study based on simulation and device physics concepts of 20 nm gate length PWFDSOI MOSFET has been presented in this paper. The potential wells are instrumental in reducing the OFF current of the device significantly. However, the reduction

in ON current is marginal, thus significantly improving  $I_{ON}/I_{OFF}$  ratio. The study was done on devices with unstrained silicon channel. However, the study is also applicable to scaled devices having strained silicon channel, thus expecting improvement in  $I_{ON}$  and  $I_{ON}/I_{OFF}$  ratio.

## References

- [1] K. Roy, S. Mukhopadhyay, H. Mahmoodi-Meimand, Leakage current mechanisms and leakage reduction techniques in deep-submicrometer CMOS circuits, *Proc. IEEE* 91 (2) (2003) 305 – 327, DOI:10.1109/JPROC.2002.808156.
- [2] P. Zheng, D. Connelly, F. Ding, T. K. Liu, FinFET Evolution Toward Stacked-Nanowire FET for CMOS Technology Scaling, *IEEE Trans. Electron Devices* 62 (12) (2015) 3945 – 3950, DOI:10.1109/TED.2015.2487367.
- [3] A. B. Sachid, M. Chen, C. Hu, FinFET With High- $\kappa$ Spacers for Improved Drive Current, *IEEE Electron Device Lett.* 37 (7) (2016) 835 – 838, DOI:10.1109/LED.2016.2572664.
- [4] W. Y. Choi, B. Park, J. D. Lee, T. K. Liu, Tunneling Field-Effect Transistors (TFETs) With Subthreshold Swing (SS) Less Than 60 mV/dec, *IEEE Electron Device Lett.* 28 (8) (2007) 743 – 745, DOI:10.1109/LED.2007.901273.
- [5] A. C. Seabaugh, Q. Zhang, Low-Voltage Tunnel Transistors for Beyond CMOS Logic, *Proc. IEEE* 98 (12) (2010) 2095 – 2110, DOI:10.1109/JPROC.2010.2070470.
- [6] H. Lu, A. Seabaugh, Tunnel Field-Effect Transistors: State-of-the-Art, *IEEE J. Electron Devices Society* 2 (4) (2014) 44 – 49, DOI:10.1109/JEDS.2014.2326622.
- [7] S. Salahuddin, S. Datta, Use of negative capacitance to provide voltage amplification for low power nanoscale devices, *Nano Lett.* 8 (2) (2008) 405 – 410, DOI:10.1021/nl071804g.
- [8] V. P. Hu, P. Chiu, A. B. Sachid, C. Hu, Negative capacitance enables FinFET and FDSOI scaling to 2 nm node, in: 2017 IEEE Int. Electron Devices Meeting (IEDM), 2017, pp. 23.1.1 – 23.1.4, DOI:10.1109/IEDM.2017.8268443.
- [9] S. Qureshi, S. Mehrotra, Potential Well Based FD-SOI MOSFET: A Novel Planar Device for 10 nm Gate Length, in: 2019 IEEE SOI-3D-Subthres. Microelectronics Tech. Unified Conf. (S3S), 2019.
- [10] Q. Liu, et al., High performance UTBB FD-SOI devices featuring 20nm gate length for 14nm node and beyond, in: 2013 IEEE Int. Electron Devices Meeting (IEDM), 2013, pp. 9.2.1 – 9.2.4, DOI:10.1109/IEDM.2013.6724592.
- [11] C. K. Jaiswal, Nishant, S. Mehrotra, S. Qureshi, Proposed Process Flow for Potential Well Based FDSOI MOSFET at 20 nm Gate Length, in: 4th IEEE Electron Devices Tech. Manufacturing (EDTM) Conf. 2020, 2020.
- [12] Atlas user's manual, device simulation software, 2015. URL <http://www.silvaco.com>.
- [13] A. Majumdar, Z. Ren, S. J. Koester, W. Haensch, Undoped-body extremely thin SOI MOSFETs with back gates, *IEEE Trans. Electron Devices* 56 (10) (2009) 2270 – 2276, DOI:10.1109/TED.2009.2028057.